Enigma interacts with adaptor protein with PH and SH2 domains to control insulin-induced actin cytoskeleton remodeling and glucose transporter 4 translocation.

Romain Barrès, Thierry Grémeaux, Philippe Gual, Teresa Gonzalez, Jean Gugenheim, Albert Tran, Yannick Le Marchand-Brustel, Jean-François Tanti

ENIGMA INTERACTS WITH APS TO CONTROL INSULIN-INDUCED ACTIN CYTOSKELETON REMODELING AND GLUT 4 TRANSLOCATION

Romain Barrès[1], Thierry Grémeaux[1], Philippe Gual[1] Teresa Gonzalez[1], Jean Gugenheim[2], Albert Tran[3], Yannick Le Marchand-Brustel[1] and Jean-François Tanti[1]§

[1]INSERM, U568, F-06107 Nice, France; Université de Nice Sophia–Antipolis, Faculté de Médecine, F-06107, Nice, France ; [2]CHU de Nice, Service de Chirurgie Digestive et Centre de Transplantation Hépatique, Nice, France; [3]CHU de Nice Fédération d'Hépatologie, Nice, France.

§ *Corresponding Author:* Jean-François Tanti
INSERM U 568,
FACULTÉ DE MÉDECINE
AVENUE DE VALOMBROSE
06107 NICE CEDEX 02, FRANCE
tanti@unice.fr
Tel: +33-4-93 37 77 99
Fax: +33-4-93 37 77 01

Abbreviated title: APS/Enigma complex and Glut 4 translocation

Key words : 3T3-L1 adipocytes, insulin signaling, glucose transport, LIM domains, cortical actin

The authors have nothing to disclose.

Abstract:

APS (Adaptor protein with PH and SH2 domains) initiates a PI 3-kinase independent pathway involved in insulin-stimulated glucose transport. We recently identified Enigma, a PDZ and LIM domain-containing protein, as a partner of APS and showed that APS/Enigma complex plays a critical role in actin cytoskeleton organization in fibroblastic cells. Since actin rearrangement is important for insulin-induced Glut 4 translocation, we studied the potential involvement of Enigma in insulin-induced glucose transport in 3T3-L1 adipocytes. Enigma mRNA was expressed in differentiated adipocytes and APS and Enigma were co-localized with cortical actin. Expression of an APS mutant unable to bind Enigma increased the insulin-induced Glut 4 translocation to the plasma membrane. By contrast, overexpression of Enigma inhibited insulin-stimulated glucose transport and Glut 4 translocation without alterations in proximal insulin signaling. This inhibitory effect was prevented with the deletion of the LIM domains of Enigma. Using time-lapse fluorescent microscopy of GFP-actin, we demonstrated that the overexpression of Enigma altered insulin-induced actin rearrangements, whereas the expression of Enigma without its LIM domains was without effect. A physiological link between increased expression of Enigma and an alteration in insulin-induced glucose uptake was suggested by the increase in Enigma mRNA expression in adipose tissue of diabetic obese patients. Taken together, these data strongly suggest that the interaction between APS and Enigma is involved in insulin-induced Glut 4 translocation by regulating cortical actin remodelling and raise the possibility that modification of APS/Enigma ratio could participate in the alteration of insulin-induced glucose uptake in adipose tissue.

INTRODUCTION

Insulin signaling is required for normal glucose homeostasis. Binding of insulin to its receptor results in the phosphorylation of several intracellular substrates, including the insulin receptor substrate (IRS) family, Shc, and APS. IRS phosphorylation leads to the activation of the PI 3 kinase pathway that is critical for insulin-induced glucose transport and Glut 4 translocation. However, while necessary the PI 3-kinase pathway does not seem to be sufficient and recently, a new pathway, independent of PI 3-kinase activation, has been described (1). This pathway requires tyrosine phosphorylation of the adaptor protein APS by the insulin receptor (2). APS for "Adaptor Protein with PH and SH2 domains" is the last identified member of a conserved family of SH2 adaptor molecules including Lnk and SH2-B (3). All members of this family contain a C-terminal SH2 domain, a central PH domain, and a N-terminal proline-rich region. Lnk is involved in T-cell receptor activation while APS and SH2-B are involved in the signaling pathway of receptors for various growth factors including insulin and IGF-1. APS is highly expressed in insulin-responsive tissues, especially in adipocytes, and is the preferential target for the insulin receptor kinase in these cell types compared to SH2-B (3, 4). APS associates with phosphotyrosine residues situated within the activation loop of the insulin receptor via its SH2 domain (4-6) and undergoes insulin-stimulated tyrosine phosphorylation on tyrosine 618 allowing it to bind Cbl in complex with CAP (7). Once phosphorylated on tyrosine residues, Cbl recruits the adapter protein CrkII in a complex with C3G, a GDP to GTP exchange factor for TC10, a Rho-family GTPase that regulates Glut 4 trafficking (1). Several data favor an important role of APS in Glut 4 translocation. Indeed, in 3T3-L1 adipocytes, expression of a Y618F mutant of APS that is not phosphorylated in response to insulin, or knock-down of APS protein expression by using siRNA strategy inhibits insulin-induced Glut 4 translocation and glucose transport (2, 8). Studies of APS-deficient mice have led to contradictory results since one report describes an increase in whole body insulin sensitivity and insulin effect on glucose transport in adipocytes while a more recent study concludes that APS does not appear to modulate insulin regulation of glucose metabolism (9, 10). Thus, in order to bring about gain of insight into function of this protein, we searched for new partners of APS and identified Enigma as an APS binding protein by yeast two-hybrid screening (11). Enigma belongs to a family of cytoplasmic proteins and structurally, contains one amino-terminal

PDZ domain and one to three carboxy-terminal LIM domains. Both PDZ and LIM domains are protein-protein interacting modules and several LIM domain-containing proteins were found to be associated with the actin cytoskeleton, playing a role in signal transduction and organization of actin filaments during various cellular processes (12-14). The LIM domains of Enigma bind to protein kinases while its PDZ domain was shown to interact with actin binding proteins such as ß-tropomyosin (13-15). This family of proteins could be involved in targeting protein kinases to cytoskeleton elements. Our recent report showing that Enigma and APS are co-localized with F-actin in insulin-induced membrane ruffles (11) and the previous report that Enigma interacts directly with the insulin receptor (16) support a model in which APS/Enigma complex could be a link between insulin signaling and actin cytoskeleton.

Several studies have revealed the importance of actin cytoskeletal organization in the regulation of insulin-induced Glut 4 translocation (1, 17) and implicated the TC10 pathway in this process (1). Since APS/Enigma complex is involved in actin organization (11), this prompted us to study the potential role of Enigma in insulin-induced Glut 4 translocation in adipocytes.

In the present study, we showed that APS and Enigma were co-localized with cortical actin in 3T3-L1 adipocytes and we propose that Enigma could play a role in insulin-induced Glut 4 translocation by regulating cortical actin dynamics.

RESULTS

APS and Enigma are co-localized with cortical actin cytoskeleton in 3T3-L1 adipocytes

We wanted to determine whether Enigma was expressed in 3T3-L1 cells and was associated with APS and actin cytoskeleton. Using a cDNA probe encoding the full-length sequence of Enigma, we detected, by Northern blot analysis, a transcript of 2.4 kb in both 3T3-L1 fibroblasts and fully differentiated 3T3-L1 adipocytes (Fig.1). Enigma mRNA expression was not markedly modified upon differentiation in adipocytes. By contrast, APS mRNA expression was up-regulated in differentiated 3T3-L1 adipocytes (Fig.1) in agreement with previously published data (4).

To determine the localization of the two proteins, 3T3-L1 adipocytes were co-transfected with both HA-Enigma and Myc-APS cDNAs and the distribution of the two proteins was studied by immunofluoresence staining using anti-HA and anti-Myc antibodies respectively, followed by confocal microscopy (Fig. 2, panels A-C). We used HA-tagged Enigma because no commercial antibody was available against Enigma and the antibody kindly provided by Dr. Gill (13) did not recognise the endogenous protein in immunofluorescence or immunoprecipitation studies. HA-Enigma was distributed at the plasma membrane and in intracellular compartments (Fig. 2A). Myc-APS was predominantly localized near the cell surface, as previously described (2) with lower levels detected in intracellular structures (Fig. 2B). An overlay of APS and Enigma staining revealed that the two proteins co-localized mainly at the plasma membrane (Fig. 2C) with partial co-localization inside the cells. APS and Enigma were previously shown to be associated with F-actin in membrane ruffles (11). In 3T3-L1 adipocytes, F-actin is mainlycortical, underlying the plasma membrane with some F-actin is present in perinuclear region (1). We next wanted to determine whether Enigma and APS were localized with F-actin. Myc-APS or HA-Enigma cDNAs was transiently transfected in 3T3-L1 adipocytes and F-actin structures were visualised following Texas-red phalloidin staining (Fig. 2, panels D-I). Phalloidin staining indicated that F-actin was mainly organized as cortical actin distributed at the periphery of the cells with some F-actin in the perinuclear region (Fig. 2, panels E, H). An overlay of both APS and Enigma staining with F-actin staining revealed a co-localization of APS and Enigma with cortical actin (Fig 2, panels F, I).

The interaction between APS and Enigma is involved in Glut 4 translocation

APS is an essential component of the CAP/Cbl pathway in the control of insulin–induced glucose uptake (2). Moreover, insulin-stimulated Glut 4 translocation in adipocytes is dependent upon cortical actin remodelling (17). We investigated whether the interaction between Enigma and APS plays a role in insulin-induced Glut 4 translocation. To this aim we used an APS mutant lacking the NTPY motif (Myc-APS[APTA]) needed for Enigma binding in NIH-3T3 fibroblasts (11). We first verified that this APS mutant did not interact with Enigma in 3T3-L1 adipocytes. We compared the ability of wild-type Myc-APS and Myc-APS[APTA] to interact with HA-Enigma by co-expressing both proteins in 3T3-L1 adipocytes. As shown in Fig. 3, wild-type Myc-APS co-precipitated with HA-Enigma while Myc-APS[APTA] did not. Insulin did not modify the interaction between APS and Enigma (data not shown). We next examined whether expression of the Myc-APS[APTA] mutant modulates insulin-stimulated Glut 4 translocation. 3T3-L1 adipocytes were electroporated with plasmids coding for GFP, GFP-APS, or GFP-APS[APTA] together with a construct coding for a DsRed protein fusion of Myc-Glut 4 (Myc-Glut 4-DsRed), and were treated without or with insulin. Myc-Glut 4-DsRed at the cell surface of co-transfected cells was detected following anti-Myc antibody and Cy5-conjugated secondary antibody binding as described (18). Only cells with a continuous Cy5 fluorescent rim were considered as positive for Glut 4 translocation. The use of a Glut4 transporter with a Myc-epitope tag allowed us to determine the amount of Glut 4 that was properly inserted in the plasma membrane with the Myc-epitope towards the extracellular medium. In basal state, the number of cells with Myc-Glut 4-DsRed at the cell surface was similar between the different conditions of transfection (Fig. 4A, left panel). The number of GFP or GFP-APS-expressing cells displaying a fluorescent rim at the cell surface was similarly increased following insulin stimulation. In contrast, the number of cells presenting a continuous fluorescent rim at the cell surface increased by 30% with the expression of GFP-APS[APTA] compared to adipocytes that expressed GFP or GFP-APS (Fig. 4A, left panel). We then determined the effect of GFP-APS[APTA]on insulin-induced glucose uptake. To this aim, 3T3-L1 adipocytes were transfected with 400 µg of vectors coding for GFP, GFP-APS or GFP-APS[APTA]. In these conditions approximately 60 to70 % of cells were actually transfected as previously shown (19) allowing for the measurement of an effect of the different constructs on glucose

uptake. Expression of GFP-APS[APTA] increased the insulin effect on glucose uptake compared to cells expressing GFP or GFP-APS (Fig. 4A, right panel). This effect was not due to a change in early steps in insulin signaling or to an increase in the amount of Glut 4 (Fig. 4B) These results indicate that Enigma binding to APS could play a role in the regulation of Glut 4 translocation and glucose uptake.

Overexpression of Enigma decreases insulin-induced Glut 4 translocation and glucose uptake in 3T3-L1 adipocytes.

The fact that the disruption of APS and Enigma interaction favored the insulin-induced Glut 4 translocation, prompted us to investigate the role of Enigma in this process. 3T3-L1 adipocytes were electroporated with plasmids coding for GFP or GFP-Enigma together with Myc-Glut 4-Dsred. The number of cells with Myc-Glut 4-DsRed at the cell surface was quantified, as described above. In basal state, the number of cells with Myc-Glut 4-DsRed at the cell surface was similar with the expression of GFP or GFP-Enigma. Importantly, following insulin stimulation, the number of cells with Myc-DsRed-Glut 4 at the cell surface was reduced by 40% with the expression of GFP-Enigma (Fig. 5A, left panel). LIM domains act as modular protein-binding domains that play an important role in the functions of LIM proteins. To determine if LIM domains of Enigma were involved in its inhibitory effect on Glut 4 translocation, we expressed GFP-Enigma without the LIM domains (GFP-ENG ΔLIM1,2,3) together with Myc-Glut 4-DsRed. The expression of GFP-ENG ΔLIM1,2,3 did not decrease insulin-induced Myc-Glut 4-DsRed localization to the plasma membrane suggesting that LIM domains are necessary for the inhibitory effect of Enigma (Fig. 5A, left panel). We then assessed whether the inhibition of insulin-induced Glut 4 translocation in cell overexpressing Enigma reduced the uptake of glucose. Insulin induced a four-fold increase in glucose uptake in control cells and Enigma expression reduced by 40% the insulin effect (Fig. 5A, right panel). We next examined whether Enigma expression altered the expression of Glut 4 and /or the early insulin receptor signal transduction. As shown in Figure 5B, Enigma expression did not significantly modify the expression of Glut 4, the insulin receptor β-subunit autophosphorylation and IRS1 tyrosine phosphorylation, or PKB and ERK activation. We also verified that Enigma expression did not modify the localization of

Myc-Glut 4-DsRed in unstimulated adipocytes since inhibition of insulin-induced Myc-Glut 4-DsRed translocation in Enigma expressing adipocytes might be due to mislocalization of this protein. Thus, we compared the subcellular localization of Myc-Glut 4-DsRed in unstimulated adipocytes that expressed GFP or GFP-Enigma by direct fluorescence and confocal microscopy. As shown in reconstituted fields (Fig. 6) Myc-Glut 4-DsRed was mainly localized in perinuclear region both in GFP and GFP-Enigma transfected adipocytes. These results indicated that Enigma expression decreased insulin-induced glucose uptake probably by inhibiting endogenous Glut 4 translocation.

Enigma overexpression blocks insulin-induced actin remodelling

Insulin stimulates cortical actin rearrangement in 3T3-L1 adipocytes that is necessary for Glut 4 translocation (17). Enigma family members have been shown to regulate actin dynamic (20-23), and Enigma overexpression induces loss of stress fibers in fibroblasts (11). The co-localization of Enigma with cortical actin in 3T3-L1 adipocytes suggests that it could play a role in actin remodeling. Because cortical actin structures in adipocytes are not as pronounced as stress fibers in fibroblasts, it is difficult to detect changes in actin organization in adipocytes following fixation. Therefore, to determine whether Enigma expression can modulate insulin-induced actin rearrangement *in vivo*, we examined the dynamic of actin rearrangements by fluorescent time-lapse microscopy in cells co-expressing a GFP-actin protein together with DsRed or Enigma expressed in fusion with DsRed. In each condition, DsRed or DsRed-Enigma expression was verified (data not shown) and cells with the same level of GFP-actin were examined. As shown in Figure 7 and in the time-lapse video (see Supplementary data), insulin stimulation of the DsRed expressing cells increased actin reorganization and large actin protrusions were formed at the plasma membrane (arrows in Fig. 7A and supplemental Movie 1). By contrast, in cells expressing DsRed-Enigma, clusters of GFP-actin were observed and insulin stimulation did not lead to the formation of these actin protrusions, suggesting that GFP-actin dynamic was blocked (Fig. 7B and supplemental Movie 2). Thus, an inhibition of insulin-induced actin remodeling in cells expressing Enigma due to an alteration in actin organization could explain the inhibition of Glut 4 translocation and glucose uptake. To further investigate this hypothesis, we

studied the effect of Enigma ΔLIM1,2,3, that did not inhibit insulin-induced Glut 4 translocation, on actin dynamic. As shown in Figure 7C and supplemental Movie 3, expression of Enigma ΔLIM1,2,3 did lead to the formation of actin clusters and did not alter insulin-stimulated GFP-actin dynamic. Taken together, these data suggest that Enigma could play a role in glucose transport by regulating the dynamic of actin cytoskeleton.

APS AND Enigma mRNAs expression in adipose tissue of obese type 2 diabetic patients

Based on the above results, we hypothesized that in insulin resistant states a change in the ratio between APS and Enigma could lead to the formation of non-productive complex leading to abnormal actin dynamic. To investigate this hypothesis, we measured APS and Enigma mRNAs expression by quantitative real-time PCR analysis in subcutaneous adipose tissue of patients with type 2 diabetes. Despite a trend towards an increase, APS gene expression was not significantly modified ($P = 0.085$) in adipose tissue of obese type 2 diabetic patients compared to control subjects (Fig. 8). By contrast, Enigma mRNA expression was 5 fold increased ($P = 0.002$) in adipose tissue of diabetic patients compared with control subjects (Fig. 8). These data indicate that the expression of APS and Enigma are differentially regulated in insulin resistant state.

DISCUSSION

We previously identified the LIM and PDZ domains containing protein Enigma as a partner of APS (11). We recently demonstrated that the APS/Enigma complex is involved in actin organization in fibroblasts (11). APS is required for insulin-induced activation of the Cbl/CAP/TC10 pathway that could be potentially involved in the regulation of actin cytoskeleton (2, 24). Cell cytoskeleton plays an important role in vesicular trafficking and several reports strongly support a role of the actin cytoskeleton in insulin-induced Glut 4 translocation (1). In this study, we show that APS and Enigma co-localize with F-actin beneath the plasma membrane in 3T3-L1 adipocytes. These findings are in agreement with our previous report that Enigma binds to APS in fibroblasts and that the APS/Enigma

complex co-localizes with F-actin. In fibroblasts or preadipocytes, F-actin is well known to form stress fibers, lamellipodia, and filipodia. However, in differentiated 3T3-L1 adipocytes, F-actin forms cortical actin that is lining the inner face of the plasma membrane (1). Thus, it is likely that the APS/Enigma complex is co-localized with cortical actin in adipocytes. A role of Enigma could thus be to target adaptor proteins or growth factor receptors to cytoskeleton allowing the regulation of cell signaling. For instance, Enigma interacts with the Ret/ptc2 via its LIM2 domain and this interaction is required for mitogenic signaling probably by targeting Ret/ptc2 to cytoskeletal elements beneath the plasma membrane (14, 25). In agreement with such a role, we found that the expression of an APS mutant unable to bind Enigma increased insulin-induced Glut 4 translocation while overexpression of Enigma alone markedly decreased both insulin-induced Glut 4 translocation and glucose uptake suggesting that the interaction between Enigma and APS could be involved in the regulation of this important metabolic effect of insulin. Interestingly, using real-time imaging techniques, we show that the expression of Enigma altered actin organization with the formation actin clusters and markedly reduced insulin-induced actin remodeling. A similar effect of Enigma on actin dynamic was reported in fibroblasts (11). Indeed, in fibroblastic cell lines, the expression of Enigma induced dramatic alteration in actin cytoskeleton morphology with loss of stress fibers and the appearance of F-actin clusters. Furthermore, in cells that overexpress RIL or FHL3, two other LIM-domain containing proteins, F-actin dynamics are markedly altered suggesting that such a phenotype could be common to several LIM domain-containing proteins (22, 26).

De novo actin polymerization may play an important role in insulin-dependent Glut 4 translocation since latrunculin, which prevents actin polymerization, has an inhibitory effect on Glut 4 translocation (17, 27, 28). Moreover, jasplakinolide markedly increases actin polymerization at both cortical and perinuclear location and inhibits insulin-induced actin dynamics and Glut 4 translocation (17). The involvement of actin dynamics in Glut 4 translocation is also suggested by the observation that unconventional myosin Myo1C is required for Glut 4 trafficking in response to insulin (29). Thus, the inhibition of insulin-induced actin remodeling induced by Enigma could explain its inhibitory effect on insulin-induced Glut 4-containing vesicles translocation to the plasma membrane. The precise mechanism involved in this effect is not clear at this moment and awaits further studies. However, our

finding that Enigma protein deleted of its LIM domain did not inhibit Glut 4 translocation and actin remodeling suggests that proteins, which interact with the LIM domains, could take part in this inhibitory effect. The LIM domains of Enigma bind some PKC isoforms (23) while its PDZ domain interacts with actin-binding protein such as β-tropomyosin (13) or α–actinin (12), two proteins known to be involved in the regulation of actin organization. Thus, it is possible that an increase in Enigma expression leads to an abnormal regulation of a LIM domain-interacting protein that regulates F-actin turnover, resulting in a profound alteration in actin rearrangement. Interestingly, we found that the expression of Enigma is markedly increased in adipose tissue of diabetic patients whereas APS expression is not modified. This dysregulation in Enigma expression could contribute to the alteration in glucose transport in insulin resistant state.

Actin cytoskeleton has been proposed to be necessary for several steps in insulin-induced glucose uptake. Indeed, the maintenance of Glut 4 storage compartment and the activation of signaling proteins involved in Glut 4 translocation are dependent on an intact actin structures (17, 27, 28, 30). Furthermore, insulin might modulate the cortical actin cytoskeleton in adipocytes to allow the tethering of Glut 4 vesicles to the plasma membrane before their docking and fusion (1, 31). Finally, it has been shown that insulin stimulated the formation of actin comet tails on Glut 4-containing vesicles that are necessary for the efficient Glut 4 translocation from its storage compartment to the plasma membrane (32). It is unlikely that inhibition of insulin signaling could explain the inhibitory effect of Enigma. Indeed, insulin-induced tyrosine phosphorylation of IRS1 and activation of PKB are not altered in Enigma-expressing cells. However, we cannot exclude that Enigma expression alters the activation of the TC10 signalling pathway but disruption of F-actin was shown to be without effect on insulin-induced Cbl tyrosine phosphorylation (17). It is also unlikely that the inhibitory effect of Enigma is due to a disruption of Glut 4 sequestration compartments since both in control adipocytes and in adipocytes that express Enigma, Glut 4 is mainly localized in a perinuclear compartment that has been shown to correspond to its intracellular sequestration compartment. Thus, one possible explanation is that Enigma by inhibiting insulin-induced actin remodeling could alter the tethering of Glut 4-containing vesicles with the plasma membrane.

We propose that Enigma by interacting with APS acts as an inhibitor of cortical actin rearrangement and that insulin modifies the interaction between APS and Enigma or the interaction between Enigma and a protein associated with its LIM domains, allowing for actin reorganization and Glut 4 translocation. The later hypothesis is the more plausible since we do not detect a change in the association between APS and Enigma following insulin stimulation (data not shown). In cells that express a mutated APS unable to bind Enigma, the increase in Glut 4 translocation could be due to a more efficient cortical actin turnover that favors the insertion of Glut 4 in the plasma membrane. Thus, by interacting with Enigma, APS could be a link between insulin signaling towards glucose transport and actin reorganization in 3T3-L1 adipocytes. Studies in other cell types support a role of APS in regulation of actin cytoskeleton. Indeed, overexpressed APS co-localized with F-actin in stimulated B cells and the increase in F-actin content following BCR stimulation is more important in APS overexpressing cells than in control cells (33). Conversely, in mast cells or B cells derived from APS deficient mice the content in F-actin was decreased (34). Interestingly, insulin stimulated glucose uptake in adipocytes isolated from $APS^{-/-}$ mice was significantly increased compared to $APS^{+/+}$ mice. While F-actin content in adipocytes from APS-deficient mice (9) has not been measured, the increase in insulin effect could be in favor of a modified cortical actin organization that facilitates insulin-induced Glut 4 insertion in the plasma membrane.

In conclusion, our study identifies Enigma as a partner of APS that is involved in F-actin dynamics in 3T3-L1 adipocytes and implies the interaction between APS and Enigma in the regulation of Glut 4 translocation in response to insulin. Thus, APS would act as a scaffolding protein that allows for the communication between different partners involved in the regulation of actin cytoskeleton organization. An imbalance between the amounts of these proteins can alter insulin-induced actin remodeling and lead to a decrease in glucose transport.

MATERIALS AND METHODS

Materials

Dulbecco's modified Eagle's medium (DMEM), fetal calf serum, and calf serum were obtained from Invitrogen SARL (Cergy Pontoise, France). Polyvinylidene difluoride (PVDF) membranes were purchased from Millipore (Bedford, MA, USA). BCA reagent was obtained from Pierce Biotechnology (Rockford, Ill., USA). Protease inhibitors were obtained from Roche Diagnostics (Mannheim, Germany). All other chemical reagents were purchased from Sigma (St. Louis, MO, USA). The anti-haemagglutinin (anti-HA) and anti-Myc antibodies were purchased from Roche Diagnostics (Mannheim, Germany) and from Santa Cruz Biotechnology (Santa Cruz, CA, USA), respectively. APS and Glut 4 antibodies were purchased from Santa Cruz Biotechnology (Santa Cruz, CA, USA). Anti-phospho-ERK and antiphospho–PKB were purchased from Cell Signaling (Cell Signaling Technology, MA, USA). Anti-phosphotyrosine antibody (clone 4G10) was purchased from UBI (Charlottesville, USA). Horseradish peroxidase-conjugated secondary antibodies and secondary antibodies coupled to Fluorescein Isothiocyanate (FITC) or Cy5 were obtained from Jackson Immunoresearch Laboratories, Inc. (West Grove, PA, USA). Texas Red-phalloidin was purchased from Molecular Probes, Inc, (Eugene, OR, USA). Enhanced chemiluminescence reagent was purchased from Perkin-Elmer Life Sciences (Boston, MA). Oligonucleotides were purchased from Eurogentec (Seraing, Belgium).

Plasmid Constructs

A plasmid encoding a C-terminal fusion protein DsRed with Myc-Glut 4 (Myc-Glut 4-Dsred) was obtained by subcloning a PCR amplification of Myc-Glut 4 (Glut 4 transporter with a Myc-epitope tag in its first extracellular loop (35)) into the Sma I restriction site of pDsRed-N (BD Biosciences Clontech), Palo Alto, CA, USA) (18). The behavior of Myc-Glut 4-DsRed is similar to that of Glut 4-GFP (18, 36). Rat Myc-APS cDNA was kindly provided by Dr. D. Ginty (The Johns Hopkins

University School of Medicine, Baltimore, Maryland). Human HA-Enigma cDNA was a gift from Dr. G. Gill (Department of Biology, University of California San Diego, La Jolla, California).

Enigma ΔLIM1/2/3 and Myc-APS[APTA] constructs were generated as described (11). Full length APS and Enigma cDNA sequences as well as sequences encoding for various mutated forms were amplified by PCR and subcloned in pEGFP-C1 or pDsRed-C1 (BD biosciences Clontech, Palo Alto, CA, USA). The plasmid DNAs were purified using Qiagen purification kit (QIAGEN SA, Courtaboeuf, France).

Physical and clinical characteristics of the study population

Six women and one man severely obese diabetic patients (age 45 ± 6 years, BMI 45 ± 8 kg/m2) were included in the present study. All patients were recruited through the department of surgery and liver transplantation where they were consulting for an elective bariatric surgery of their obesity. Diabetes was diagnosed before the bariatric surgery program (fasting plasma glucose >7mmol/l or previously known diabetes). Before surgery, fasting blood samples were obtained and used for determination of glycemia (8 ± 3 mmol/L) and insulinemia (11 ± 6 mIU/L) (37). In addition, subcutaneous adipose tissue from 7 lean women (age 51 ± 10 years, BMI 22 ± 1 kg/m2), obtained while undergoing lipectomy for cosmetic purpose, was used as control adipose tissue (provided by Drs Alessi and Casanova, Marseille, France). During surgery, a surgical biopsy of subcutaneous adipose tissues was collected. Samples of the biopsies were immediately frozen in liquid nitrogen and stored at –80°C. The experimental protocol was performed according to French legislation regarding Ethic and Human Research (Huriet-Serusclat law, DGS 2003/0395). Informed consent was obtained from all obese subjects as well as from lean subjects.

Cell Culture

3T3-L1 fibroblasts were grown in 35 or 100-mm dishes in DMEM, 25 mM glucose, 10 % calf serum and induced to differentiate in adipocytes as described previously (38). Briefly, 2 days after confluence, medium was changed for DMEM, 25 mM glucose, 10 % Fetal Calf Serum (FCS) supplemented with isobutylmethylxanthine (0.25 mM), dexamethasone (0.25 mM), TZD (10 μM) and

insulin (5 µg/ml). The medium was removed after 2 days and replaced with DMEM, 25 mM glucose, 10 % FCS supplemented with insulin for two other days. The cells were then fed every two days with DMEM, 25 mM glucose, 10% FCS. 3T3-L1 adipocytes were used 8-15 days after the beginning of the differentiation protocol. Sixteen hours before each experiment, the medium was changed to serum-free DMEM supplemented with 0.5 % bovine serum albumin (BSA).

Northern Blot

Northern blot analysis was performed on poly(A)+ RNA prepared from either 3T3-L1 fibroblasts or adipocytes. A [α-^{32}P]dCTP-labeled probe corresponding to the coding sequences of APS or Enigma was generated by random priming and hybridization was performed overnight at 60°C in 15 % formamide, 1 % BSA, 0.5 M sodium phosphate (pH 7.2), 7% SDS, 100 µM EDTA, and 50 µg/ml denatured salmon sperm DNA and washed at a high stringency.

3T3-L1 Adipocytes Transfection and Glut 4 Translocation Assay

3T3-L1 adipocytes were transfected using a low voltage electroporation technique as described previously (39, 40). Briefly, At day six to sevenafter the beginning of the differentiation protocol, 3T3-L1 adipocytes grown on 10 cm tissue culture dishes were trypsinized and resuspended in DMEM at a concentration of $2x10^7$ cells/ml. Cells were mixed with 75 µg of a plasmid coding for Myc-Glut 4-DsRed and empty plasmid (75 µg) or plasmid coding for GFP-Enigma wt, GFP-Enigma ΔLIM1,2,3, GFP-APS wt or -APS[APTA] (final volume 500 µl) and electroporation was performed with an electric pulse (160V, 960 µF) using an Easyject electroporator system (Equibio, Ashford, UK). Cells were then plated on collagen IV-coated glass coverslips and allowed to recover for 20 h in complete medium. Thereafter, 3T3-L1 adipocytes were incubated for 2 h at 37 C in DMEM containing 0.1 % fetal bovine serum and then either left untreated or stimulated with insulin (100 nM) for 45 min at 37 C. The cells were washed once with ice-cold PBS and fixed with 4% paraformaldehyde (Electron Microscopy Sciences, Ft. Washington, PA) for 10 min at room temperature. After being washed, the cells were blocked with PBS, 5% bovine serum albumin and incubated with anti-Myc antibodies for 90

min at 37 C. Following washes, cells were incubated with Cy5-conjugated donkey secondary antibody (Jackson Immunoresearch Laboratories, West Grove, PA) for 60 min at room temperature. Cells were then washed twice with ice–cold PBS and coverslips were mounted in Mowiol onto glass slides. Cells were examined using a Leica confocal microscope equipped with a Leica confocal laser scanning imaging. Quantification of the number of cells displaying a Cy5-fluorescent rim was determined from counting at least 100 cells that co-expressed both Myc-Glut 4-Dsred and the different GFP constructs from at least three independent experiments. Co-transfected cells with a continuous fluorescent rim are considered positive for Glut 4 translocation. By contrast, they are considered negative when the labeling is absent, discontinuous, or when it appears as punctuate structures (18).

Confocal Immunofluorescence Microscopy

3T3-L1 adipocytes were transfected by electroporation and plated on collagen IV-coated glass cover slips as described above. After 48 h, cells were washed with ice-cold PBS and fixed in 4 % paraformaldehyde for 20 minutes at 4 C. After two washes with ice-cold PBS, cells were permeabilized with PBS containing 0.1 % Triton X-100, and 1 % BSA for 30 min at room temperature. After three washes with ice-cold PBS, cells were incubated for 2 h at room temperature with the appropriate primary antibodies in PBS/0.1% Triton X-100/1% BSA. Following washes, cells were incubated with secondary antibodies coupled to FITC or Cy5 fluorochromes and Texas Red-phalloidin in PBS/0.1 % Triton X-100/1 % BSA for 30 min at room temperature. Cells were then washed twice with ice-cold PBS and cover slips were mounted in Mowiol onto glass slides. Cells were examined using a Leica confocal microscope equipped with a Leica confocal laser scanning imaging. Cells were studied using a PL APO 63 X 1.40 oil immersion objective. Series of images were collected along the z-axis and examined by sequential excitation at 488 nm (FITC), 568 nm (Texas Red), and 647 nm (Cy5). Each experiment was repeated at least three times. The images were then analyzed using PHOTOSHOP® software (Adobe® Systems, Mountain View, CA).

2-Deoxyglucose Uptake

3T3-L1 adipocytes were transfected by electroporation with 400 µg of plasmids and plated on 12-well plates coated with collagen IV and allowed to recover for 20 h (39, 40). Thereafter, cells were serum-starved in DMEM supplemented with 0.1 % fetal bovine serum for 2 h. Cells were then washed with Krebs-Ringer phosphate buffer (10 mM phosphate buffer, pH 7.4, 1 mM $MgSO_4$, 1 mM $CaCl_2$, 136 mM NaCl, 4.7 mM KCl) and incubated without or with insulin (100 nM) for 20 min in Krebs-Ringer phosphate buffer supplemented with 0.1 % bovine serum albumin. Glucose transport was determined by the addition of 2-[^{3}H]deoxyglucose (0.1 mM, 0.5 µCi/ml) as described previously (41). The reaction was stopped after 3 min by aspiration, and cells were washed four times with ice-cold PBS. Cells were lysed in Krebs-Ringer phosphate, 1% Triton X-100, and glucose uptake was assessed by scintillation counting. Results were normalized for protein amount that was measured by BCA assay.

Immunoprecipitation and Immunoblot Analysis

Immunoprecipitation was performed as described (38). Cells were washed with ice-cold buffer (20 mM Tris, pH 7.4, 150 mM NaCl, 5 mM EDTA) before solubilisation for 30 min at 4 C in lysis buffer (20 mM Tris, pH 7.4, 150 mM NaCl, 5 mM EDTA, protease inhibitors, and 1 % Triton X-100). Following centrifugation at 15 000 x *g* for 15 min at 4 C, cell lysates were incubated for 3 h at 4 C with 4 µg of appropriate antibodies pre-adsorbed on protein G-Sepharose. The beads were washed twice with high-salt buffer (20 mM Tris, pH 7.4, 500 mM NaCl, 5 mM EDTA, protease inhibitors, and 1% Triton X-100), and once with lysis buffer. Immune pellets were boiled for 5 min in Laemmli buffer. Proteins were resolved by SDS-PAGE using 7.5 or 10% gels and were transferred to PVDF membrane. The membrane was blocked with saline buffer (10 mM Tris, pH 7.4, 140 mM NaCl) containing 5% (w/v) BSA and 0.1 % Nonidet-P40 for 2 h at room temperature, and was incubated overnight at 4 C with the indicated antibody. Following incubation with horseradish peroxidase-conjugated secondary antibodies, proteins were detected by enhanced chemiluminescence.

Time-lapse Microscopy

3T3-L1 adipocytes were transfected by electroporation with GFP-Actin with or without DsRed-Enigma or DsRed-Enigma ΔLIM1,2,3, plated on glass bottom 35 mm microwell dishes (MatTek

corporation, Ashland, MA, USA), and allowed to recover for 20 h. Thereafter, cells were stimulated by 100 nM insulin, filmed for 2 h under constant conditions (5% CO_2, 37°C) and observed by fluorescence using fully motorized Axiovert 200 microscope (Carl Zeiss, Göttingen, Germany) and a cooled, digital charge-coupled device camera (Roper Scientific, Evry, France) using a 20× lens. Images were recorded at 1 frame/1 min and processed using MetaMorph 2.0 image analysis software (Universal Imaging, Downingtown, PA) and Adobe Premiere pro® software ((Adobe® Systems, Mountain View, CA).

Analysis of mRNA expression by Real-time Quantitative PCR

Total RNAs from subcutaneous white adipose tissues were prepared using Trizol reagent (Life Technologies Inc, UK). The integrity of the RNA was confirmed by electrophoresis in ethidium bromide containing agarose gels and the RNA concentration was determined spectrophotometrically. cDNA was synthesized using MMLV transcriptase (Invitrogen) from 1 µg of total RNA. Real-time quantitative PCR reactions were performed starting with 5 µl of 1/10 dilution of the reverse transcribed cDNAs, in a final volume of 20 µl PCR reaction, with 0.5 µM of each primer using 1X TAQ MAN Master mix in an AbiPrism 7700 Sequence Detection System instrument and software (Applied Biosystems). The PCR conditions were: 2 min at 50°C, 10 min at 95°C followed by forty cycles of a two-step PCR reaction denaturation at 95°C for 15 s and annealing extension at 60°C for 60 s. A control without cDNA was performed for each experiment. The number of cycles (CT) required for the fluorescence to reach a threshold limit was determined in duplicate for each sample. The relative amounts of the different mRNAs were quantified by using the second derivative maximum method. RPLP0 was used as an invariant control, and the relative quantification for a given gene was corrected to RPLP0 mRNA values. The results were expressed relative to the control condition, which was arbitrary assigned a value of 1. For each target an efficiency of the PCR method between 95 and 100%, a reproducibility of Ct values with a standard error less than 3% and a linear range of covering more at least 7 log units were obtained. Amplification of specific transcripts was confirmed by melting curve profiles generated at the end of each run.

Pre –designed primers were from Applied Biosystem with the following assay ID:

RPLP0:Hs99999902_m1; APS:Hs00184134_m1; Enigma:hs00193775_m1.

Statistical Analysis

All data are presented as means ± SEM. The statistical comparison between experimental conditions was carried out using Student's *t*-test. A *P* values < 0.05 were considered significant.

Acknowledgments

This work was supported by grants from INSERM (France), the University of Nice, the Fondation Bettencourt-Schueller, the Fondation pour la Recherche Médicale, the Région Provence-Alpes Côte d'Azur, the Conseil Général des Alpes Maritimes, and the Association pour la Recherche Contre le Cancer (Grant 7449). J-F Tanti is supported by CNRS (France). YLMB was the recipient of an interface grant from CHU of Nice. P Gual was the recipient of a French Research Ministry grant (ACI JC5327). We are grateful to Drs DD.Ginty and GN.Gill for the gift of the different plasmids. We thank J. Vukmirica for critical reading of the manuscript and M. Cormont for helpful discussion of the data and for time-lapse videomicroscopy experiments.

References

1. Watson RT, Kanzaki M, Pessin JE 2004 Regulated membrane trafficking of the insulin-responsive glucose transporter 4 in adipocytes. Endocr Rev 25:177-204
2. Liu J, Kimura A, Baumann CA, Saltiel AR 2002 APS facilitates c-Cbl tyrosine phosphorylation and GLUT4 translocation in response to insulin in 3T3-L1 adipocytes. Mol Cell Biol 22:3599-3609
3. Yokouchi M, Suzuki R, Masuhara M, Komiya S, Inoue A, Yoshimura A 1997 Cloning and characterization of APS, an adaptor molecule containing PH and SH2 domains that is tyrosine phosphorylated upon B-cell receptor stimulation. Oncogene 15:7-15
4. Moodie SA, Alleman-Sposeto J, Gustafson TA 1999 Identification of the APS protein as a novel insulin receptor substrate. J Biol Chem 274:11186-11193
5. Ahmed Z, Smith BJ, Pillay TS 2000 The APS adapter protein couples the insulin receptor to the phosphorylation of c-Cbl and facilitates ligand-stimulated ubiquitination of the insulin receptor. FEBS Lett 475:31-34
6. Hu J, Liu J, Ghirlando R, Saltiel AR, Hubbard SR 2003 Structural basis for recruitment of the adaptor protein APS to the activated insulin receptor. Mol Cell 12:1379-1389
7. Ahmed Z, Smith BJ, Kotani K, Wilden P, Pillay TS 1999 APS, an adapter protein with a PH and SH2 domain, is a substrate for the insulin receptor kinase. Biochem J 341 (Pt 3):665-668
8. Ahn MY, Katsanakis KD, Bheda F, Pillay TS 2004 Primary and essential role of the adaptor protein APS for recruitment of both c-Cbl and its associated protein CAP in insulin signaling. J Biol Chem 279:21526-21532
9. Minami A, Iseki M, Kishi K, Wang M, Ogura M, Furukawa N, Hayashi S, Yamada M, Obata T, Takeshita Y, Nakaya Y, Bando Y, Izumi K, Moodie SA, Kajiura F, Matsumoto M, Takatsu K, Takaki S, Ebina Y 2003 Increased insulin sensitivity and hypoinsulinemia in APS knockout mice. Diabetes 52:2657-2665
10. Li M, Ren D, Iseki M, Takaki S, Rui L 2006 Differential Role of SH2-B and APS in Regulating Energy and Glucose Homeostasis. Endocrinology 147: 2163-2170
11. Barres R, Gonzalez T, Marchand-Brustel YL, Tanti JF 2005 The interaction between the adaptor protein APS and Enigma is involved in actin organisation. Exp Cell Res 308:334-344
12. Khurana T, Khurana B, Noegel AA 2002 LIM proteins: association with the actin cytoskeleton. Protoplasma 219:1-12
13. Guy PM, Kenny DA, Gill GN 1999 The PDZ domain of the LIM protein enigma binds to beta-tropomyosin. Mol Biol Cell 10:1973-1984
14. Durick K, Wu RY, Gill GN, Taylor SS 1996 Mitogenic signaling by Ret/ptc2 requires association with enigma via a LIM domain. J Biol Chem 271:12691-12694
15. Wu RY, Gill GN 1994 LIM domain recognition of a tyrosine-containing tight turn. J Biol Chem 269:25085-25090
16. Wu R, Durick K, Songyang Z, Cantley LC, Taylor SS, Gill GN 1996 Specificity of LIM domain interactions with receptor tyrosine kinases. J Biol Chem 271:15934-15941
17. Kanzaki M, Pessin JE 2001 Insulin-stimulated GLUT4 translocation in adipocytes is dependent upon cortical actin remodeling. J Biol Chem 276:42436-42444
18. Mari M, Monzo P, Kaddai V, Keslair F, Gonzalez T, Le Marchand-Brustel Y, Cormont M 2006 The Rab4 effector Rabip4 plays a role in the endocytotic trafficking of Glut 4 in 3T3-L1 adipocytes. J Cell Sci 119:1297-1306
19. Chiang SH, Baumann CA, Kanzaki M, Thurmond DC, Watson RT, Neudauer CL, Macara IG, Pessin JE, Saltiel AR 2001 Insulin-stimulated GLUT4 translocation requires the CAP-dependent activation of TC10. Nature 410:944-948
20. Arber S, Hunter JJ, Ross J, Jr., Hongo M, Sansig G, Borg J, Perriard JC, Chien KR, Caroni P 1997 MLP-deficient mice exhibit a disruption of cardiac cytoarchitectural organization, dilated cardiomyopathy, and heart failure. Cell 88:393-403
21. Bauer K, Kratzer M, Otte M, de Quintana KL, Hagmann J, Arnold GJ, Eckerskorn C, Lottspeich F, Siess W 2000 Human CLP36, a PDZ-domain and LIM-domain protein, binds to

alpha-actinin-1 and associates with actin filaments and stress fibers in activated platelets and endothelial cells. Blood 96:4236-4245

22. Coghill ID, Brown S, Cottle DL, McGrath MJ, Robinson PA, Nandurkar HH, Dyson JM, Mitchell CA 2003 FHL3 is an actin-binding protein that regulates alpha-actinin-mediated actin bundling: FHL3 localizes to actin stress fibers and enhances cell spreading and stress fiber disassembly. J Biol Chem 278:24139-24152
23. Dawid IB, Breen JJ, Toyama R 1998 LIM domains: multiple roles as adapters and functional modifiers in protein interactions. Trends Genet 14:156-162
24. Saltiel AR, Pessin JE 2002 Insulin signaling pathways in time and space. Trends Cell Biol 12:65-71
25. Durick K, Gill GN, Taylor SS 1998 Shc and Enigma are both required for mitogenic signaling by Ret/ptc2. Mol Cell Biol 18:2298-2308
26. Vallenius T, Scharm B, Vesikansa A, Luukko K, Schafer R, Makela TP 2004 The PDZ-LIM protein RIL modulates actin stress fiber turnover and enhances the association of alpha-actinin with F-actin. Exp Cell Res 293:117-128
27. Tsakiridis T, Vranic M, Klip A 1994 Disassembly of the actin network inhibits insulin-dependent stimulation of glucose transport and prevents recruitment of glucose transporters to the plasma membrane. J Biol Chem 269:29934-29942
28. Omata W, Shibata H, Li L, Takata K, Kojima I 2000 Actin filaments play a critical role in insulin-induced exocytotic recruitment but not in endocytosis of GLUT4 in isolated rat adipocytes. Biochem J 346 Pt 2:321-328
29. Bose A, Robida S, Furcinitti PS, Chawla A, Fogarty K, Corvera S, Czech MP 2004 Unconventional myosin Myo1c promotes membrane fusion in a regulated exocytic pathway. Mol Cell Biol 24:5447-5458
30. Tsakiridis T, Tong P, Matthews B, Tsiani E, Bilan PJ, Klip A, Downey GP 1999 Role of the actin cytoskeleton in insulin action. Microsc Res Tech 47:79-92
31. Watson RT, Furukawa M, Chiang SH, Boeglin D, Kanzaki M, Saltiel AR, Pessin JE 2003 The exocytotic trafficking of TC10 occurs through both classical and nonclassical secretory transport pathways in 3T3L1 adipocytes. Mol Cell Biol 23:961-974
32. Kanzaki M, Watson RT, Khan AH, Pessin JE 2001 Insulin stimulates actin comet tails on intracellular GLUT4-containing compartments in differentiated 3T3L1 adipocytes. J Biol Chem 276:49331-49336
33. Iseki M, Kubo C, Kwon SM, Yamaguchi A, Kataoka Y, Yoshida N, Takatsu K, Takaki S 2004 Increased numbers of B-1 cells and enhanced responses against TI-2 antigen in mice lacking APS, an adaptor molecule containing PH and SH2 domains. Mol Cell Biol 24:2243-2250
34. Kubo-Akashi C, Iseki M, Kwon SM, Takizawa H, Takatsu K, Takaki S 2004 Roles of a conserved family of adaptor proteins, Lnk, SH2-B, and APS, for mast cell development, growth, and functions: APS-deficiency causes augmented degranulation and reduced actin assembly. Biochem Biophys Res Commun 315:356-362
35. Cormont M, Bortoluzzi MN, Gautier N, Mari M, van Obberghen E, Le Marchand-Brustel Y 1996 Potential role of Rab4 in the regulation of subcellular localization of Glut4 in adipocytes. Mol Cell Biol 16:6879-6886.
36. Dobson SP, Livingstone C, Gould GW, Tavare JM 1996 Dynamics of insulin-stimulated translocation of GLUT4 in single living cells visualised using green fluorescent protein. FEBS Lett 393:179-184.
37. Anty R, Beckri S, Luciani N, Saint-Paul M-C, Dahman M, Iannelli A, Ben Amor I, Staccini-Myx A, Huet P-M, Gugenheim J, Sadoul J-L, Le Marchand-Brustel Y, Tran A, Gual P 2006 The inflammatory C-reactive protein is increased in both liver and adipose tissue in severely obese patients indenpendently from metabolic syndrome, type 2 diabetes and NASH. American Journal of Gastroenterology 101:1-10
38. Gual P, Gonzalez T, Grémeaux T, Barrès R, Le Marchand-Brustel Y, Tanti JF 2003 Hyperosmotic stress inhibits insulin receptor substrate-1 function by distinct mechanisms in 3T3-L1 adipocytes. J Biol Chem 278:26550-26557

39. Watson RT, Pessin JE 2000 Functional cooperation of two independent targeting domains in syntaxin 6 is required for its efficient localization in the trans-golgi network of 3T3L1 adipocytes. J Biol Chem 275:1261-1268.
40. Okada S, Mori M, Pessin JE 2003 Introduction of DNA into 3T3-L1 adipocytes by electroporation. Methods Mol Med 83:93-96
41. Tanti JF, Gremeaux T, van Obberghen E, Le Marchand-Brustel Y 1994 Serine/threonine phosphorylation of insulin receptor substrate 1 modulates insulin receptor signaling. J Biol Chem 269:6051-6057

Figure legends

Fig. 1. Expression of Enigma and APS in 3T3-L1 adipocytes

Northern blot containing poly(A)+ RNA from 3T3-L1 fibroblasts or adipocytes was hybridized with Enigma, APS or GAPDH probes. The arrows on the right denote the position of the Enigma, APS and GAPDH transcripts. A typical Northern blot representative of two independent experiments is shown

Fig. 2. APS and Enigma are co-localized with cortical actin cytoskeleton in 3T3-L1 adipocytes

3T3-L1 adipocytes were seeded on coverslips after transfection with plasmid coding for HA-Enigma or Myc-APS. Following fixation and permeabilization, cells were co-stained with anti-Myc antibody to detect APS (panel B, D), anti-HA antibody to detect Enigma (panels A, G), and, Texas Red-conjugated phalloidin to detect F-actin (panels E, H) and analyzed by confocal immunofluorescence microscopy. The merge images are shown in the panels C, F, I. Representative cells from three to four independent experiments are shown.

Fig. 3. Deletion of the APTA motif of APS prevents the interaction with Enigma in 3T3-L1 adipocytes

3T3-L1 adipocytes were electroporated with Myc-APSwt alone or co-transfected with HA-Enigma and Myc-APS or Myc-APS[APTA]. HA-Enigma was immunoprecipitated from cell lysates with anti-HA antibody and immunoprecipitates were blotted with anti-Myc antibody. The level of expression of HA-Enigma and Myc-APS or Myc-APS[APTA] was controlled following immunoblotting with anti-HA antibody or anti-Myc antibody respectively. Representative autoradiographs from three independent experiments are shown

Fig. 4. Overexpression of APS[APTA] increases insulin-stimulated Glut 4 translocation and glucose uptake

(A) *left panel* 3T3-L1 adipocytes were electroporated with 75 µg of Myc-Glut 4-DsRed cDNA together with 75 µg of GFP, GFP-APS, or GFP-APS[APTA] cDNAs. The cells were allowed to

recover for 20 h, then were serum-starved for 2 h and subsequently treated without or with 100 nM insulin for 45 min at 37 C. Cells were fixed and incubated with anti-Myc antibody and anti-mouse Cy5-conjugated antibody. Co-transfected cells were analyzed for the presence of a visually detectable plasma membrane (PM) fluorescent rim as described in Material and Methods. These data represent scoring of at least 100 cells from four independent experiments. Each bar represents an average number of co-transfected cells displaying cell surface fluorescence $\pm$ SEM (* $P < 0.05$). *right panel***,** 3T3-L1 adipocytes were electroporated with 400 µg of GFP, GFP-APS or GFP-APS[APTA] cDNAs. Cells were allowed to recover and left untreated or stimulated with insulin (100 nM) for 20 min at 37 C. Uptake of [2-^{3}H]deoxyglucose (2-DOG) was measured during a 3-min period as described in "Material and Methods". Means $\pm$ SEM from three independent experiments are shown (* $P < 0.01$). **(B)** 3T3-L1 adipocytes were electroporated as described above and left untreated or stimulated with insulin (100 nM) for 5 min at 37 C. Western blot shows 3T3-L1 adipocyte lysates blotted with phospho tyrosine, phospho PKB (Ser473), phospho ERK (T202/Y204), or Glut 4 antibodies. GFP-APS or GFP-APS[APTA] expression was visualized with anti-GFP antibody. Representative autoradiographs from three independent experiments are shown

Fig. 5. Enigma overexpression inhibits insulin-stimulated Glut 4 translocation and glucose transport in 3T3-L1 adipocytes

(A) *left panel,* 3T3-L1 adipocytes were electroporated with 75 µg of Myc-Glut 4-DsRed cDNA together with 75 µg of GFP, GFP-Enigma, or GFP-EnigmaΔLIM1,2,3 cDNAs. The cells were allowed to recover for 20 h, then were serum-starved for 2 h and subsequently treated without or with 100 nM insulin for 40 min at 37 C. Cells were fixed and incubated with anti-Myc antibody and anti-mouse Cy5-conjugated antibody. Transfected cells displaying visually detectable plasma membrane (PM) rim fluorescence were detected by indirect immunofluorescence. These data represent scoring of at least 100 cells from four to five independent experiments. Each bar represents an average number of co-transfected cells displaying cell surface fluorescence $\pm$ SEM (* $P < 0.05$). *right panel,* 3T3-L1

adipocytes were electroporated with 400 µg of GFP or with 400 µg GFP-Enigma cDNA. Cells were allowed to recover and left untreated or stimulated with insulin (100 nM) for 20 min at 37 C. Uptake of [2-^{3}H]deoxyglucose (2-DOG) was measured during a 3-min period as described in "Material and Methods". Means ± SEM from three independent experiments are shown (* $P < 0.01$). **(B)** 3T3-L1 adipocytes were electroporated with 400 µg of GFP or GFP-Enigma cDNAs and cells were allowed to recover for 20 h and then incubated in serum-free media for 4 h. Cells were subsequently left untreated or stimulated with insulin (1 or 100 nM) for 5 min at 37 C. Proteins from cell lysate were subjected to Western blotting with monoclonal phosphotyrosine antibody to analyze IRS and IR tyrosine phosphorylation. PKB and ERK activation were analyzed with anti-phospho PKB (Ser473) and anti-phospho ERK (T202/Y204), respectively. Glut 4 and GFP-Enigma expression were visualized with anti-Glut 4 or anti-GFP antibody respectively. Representative autoradiographs from three independent experiments are shown

Fig.6. Myc-Glut 4-DsRed localization in 3T3-L1 adipocytes expressing Enigma

3T3-L1 adipocytes were transfected with Myc-Glut 4-DsRed and GFP or GFP-Enigma cDNAs. Cells were fixed and localization of Myc-Glut 4-Dsred in co-transfected cells was analyzed by direct fluorescence and confocal microscopy. Reconstituted fields are shown.

Fig.7. Enigma expression altered insulin-induced actin rearrangements

3T3-L1 adipocytes were transfected with a plasmid encoding for GFP-actin together with DsRed (A and supplemental video1), DsRed-Enigma (B and supplemental video2) or DsRed-EnigmaΔLIM1,2,3 (C and supplemental video3) cDNAs. The cells were then continuously visualized by time-lapse fluorescent microscopy. Selected time images prior (0 min) and subsequent to the addition of insulin (10-180 min) are presented. The complete time-lapse films are provided in Supplemental Data section. This is a representation of insulin-stimulated time course of GFP-actin observed in three individual experiments.

Fig.8. Enigma mRNA expression is increased in adipose tissue of diabetic patients

Total RNA was extracted from subscutaneous adipose tissue biopsies from control (empty bars) of obese and diabetic patients (black bars) and the amount of APS and Enigma mRNAs was quantified by real-time quantitiative PCR . mRNA expression was normalized using RPLP0 RNA levels. Results are the means $\pm$ SEM of n=7 for each group. *, P = 0.002; ns, non significant.

Fig 1.

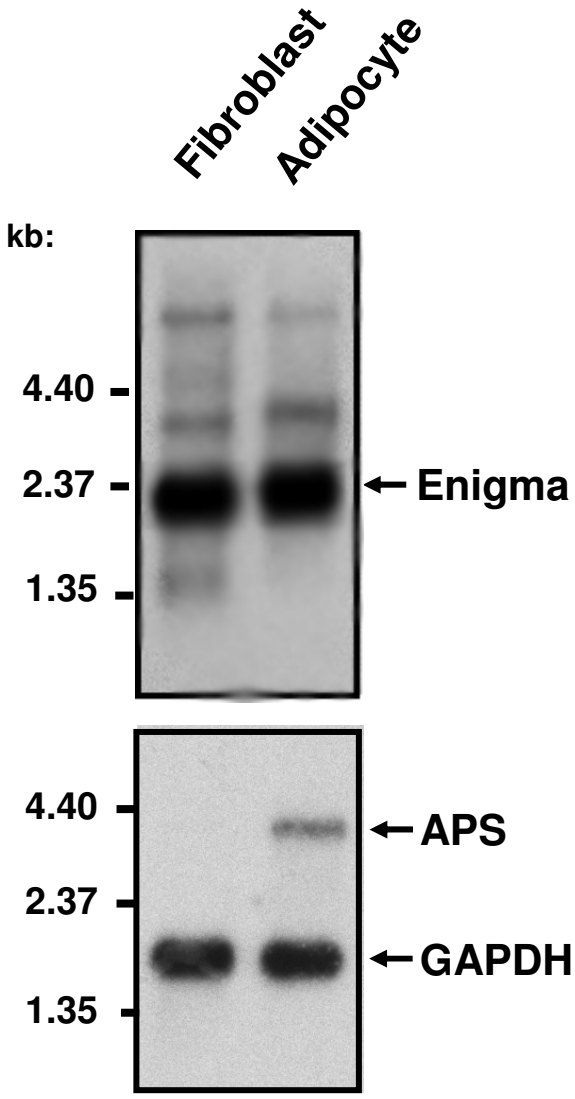

Fig 2.

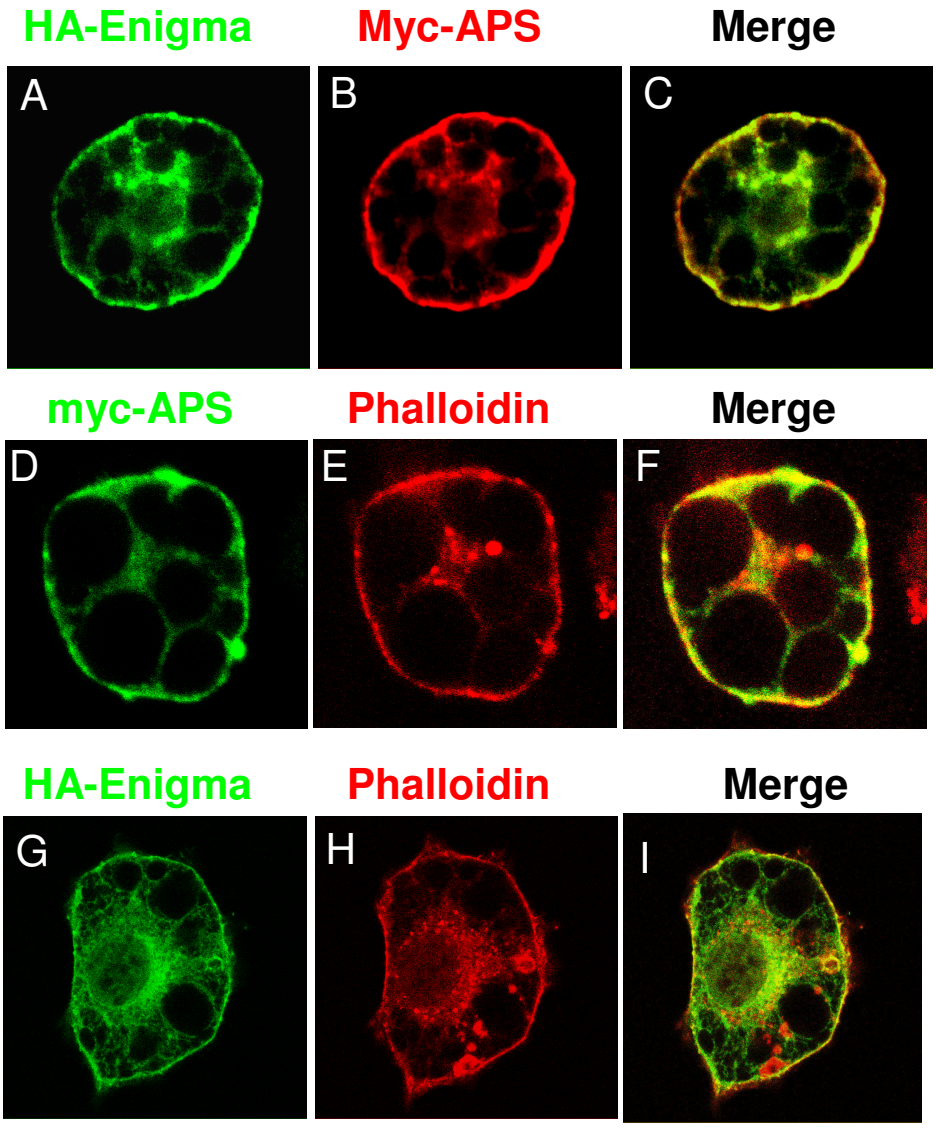

Fig 3.

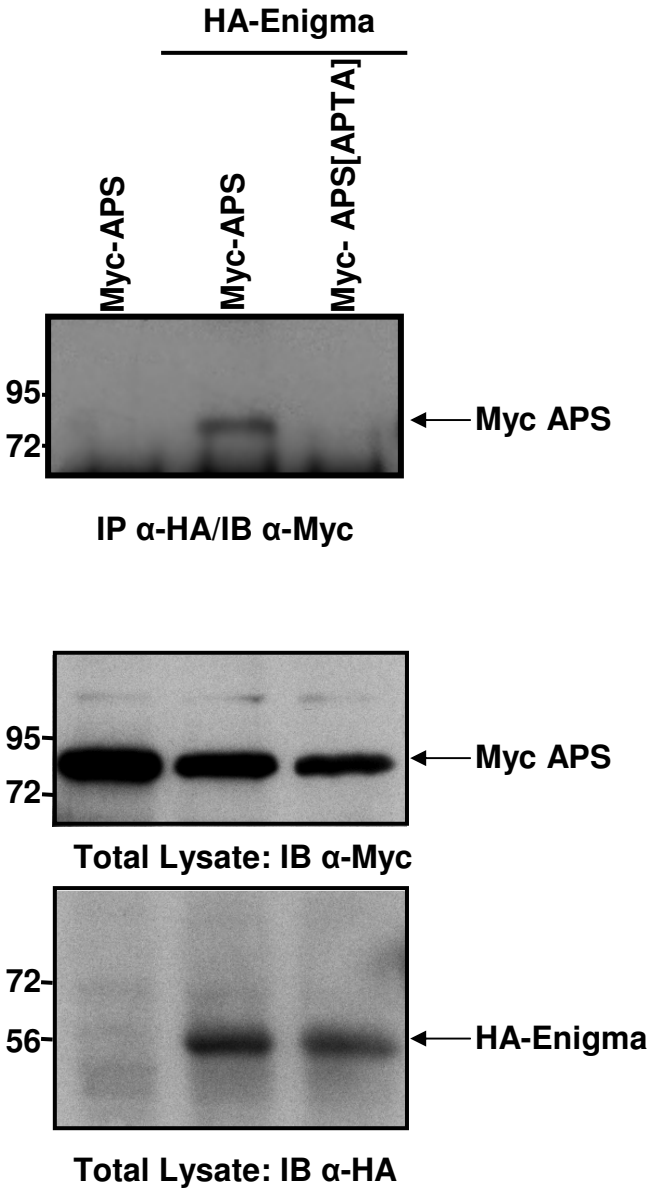

Fig 4.

A

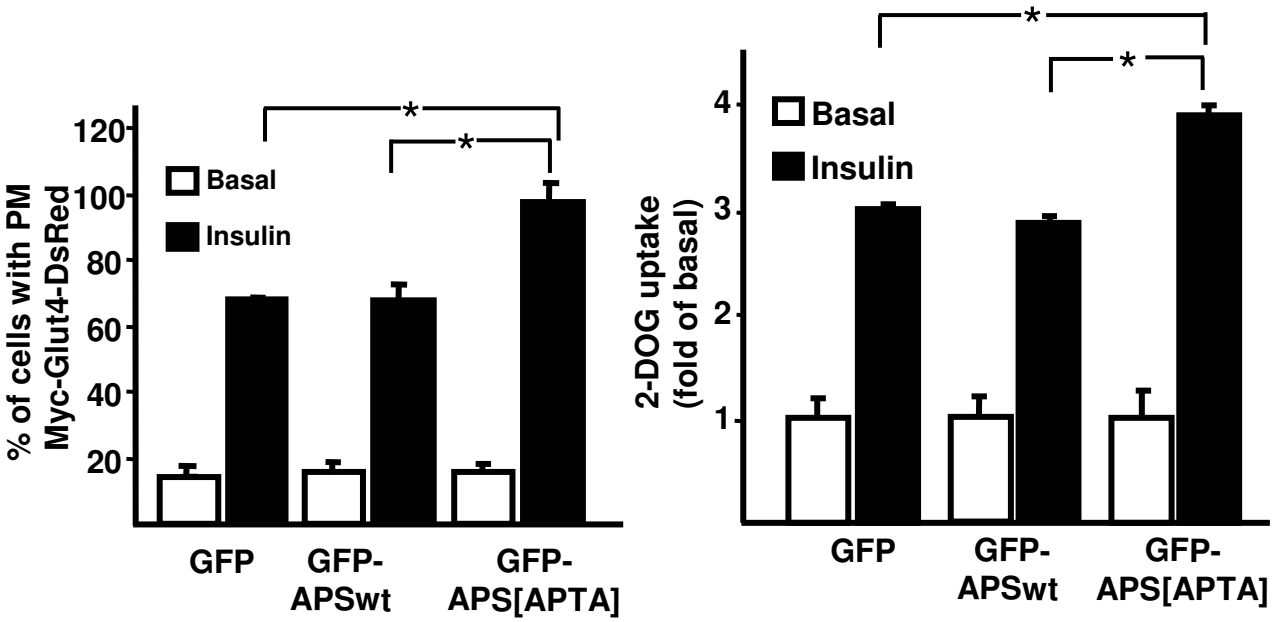

B

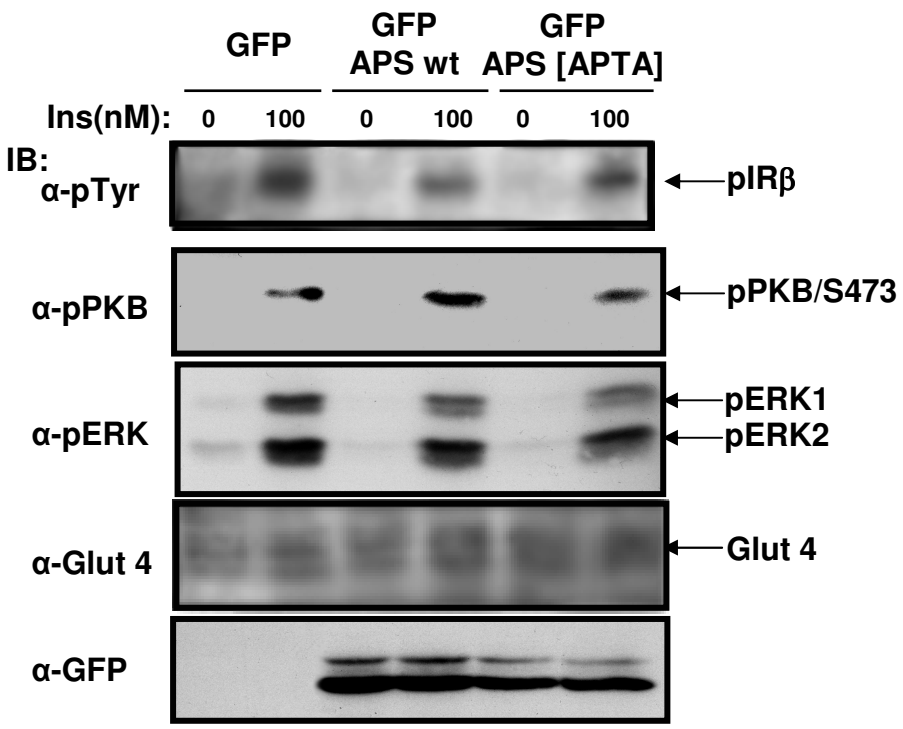

Fig 5.

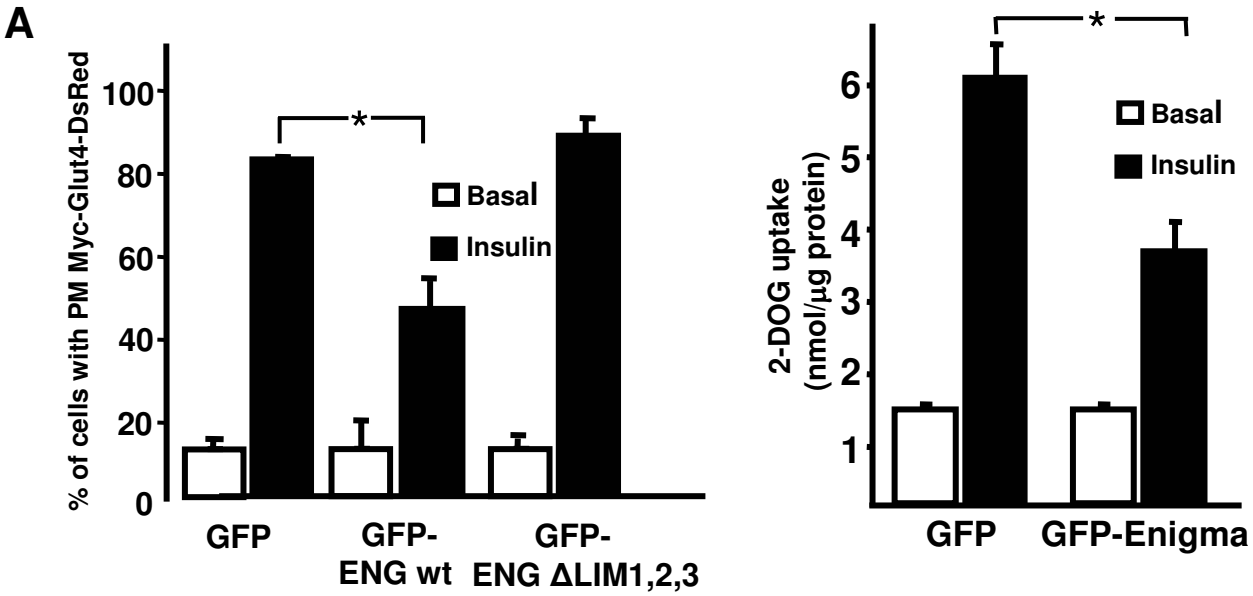

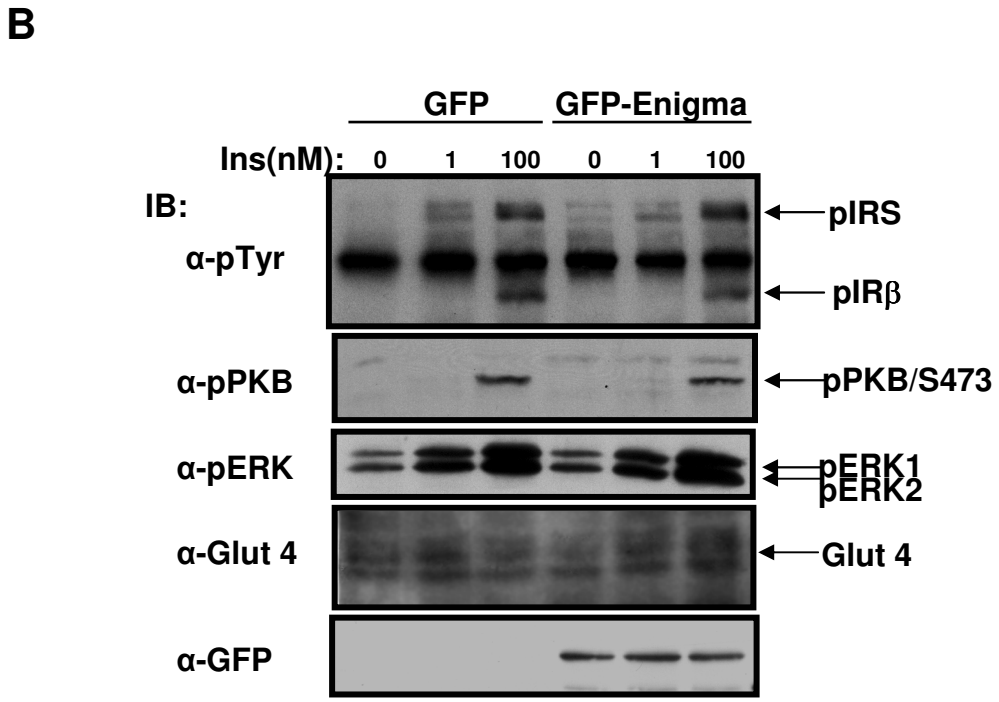

Fig 6.

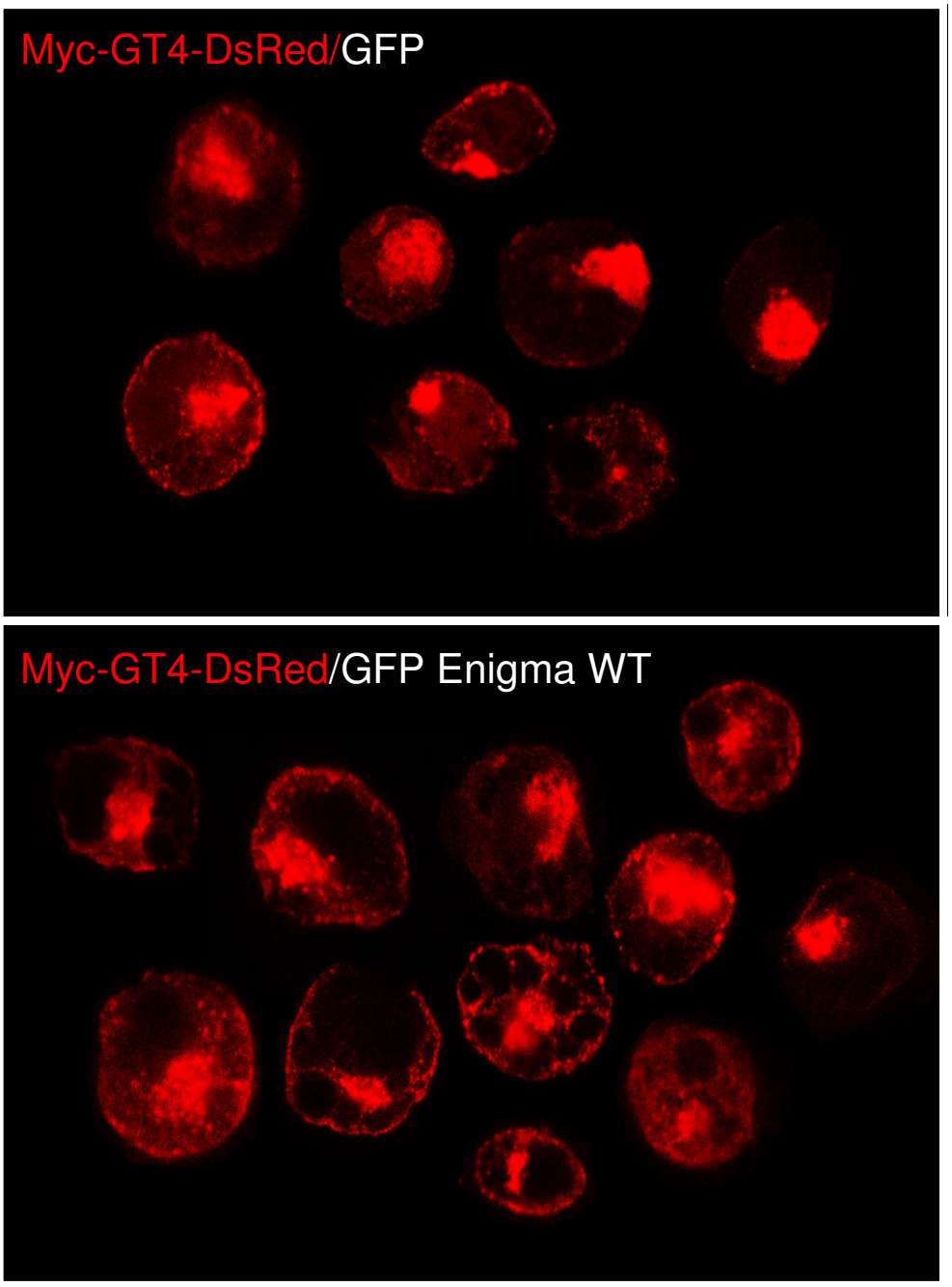

Fig 7.

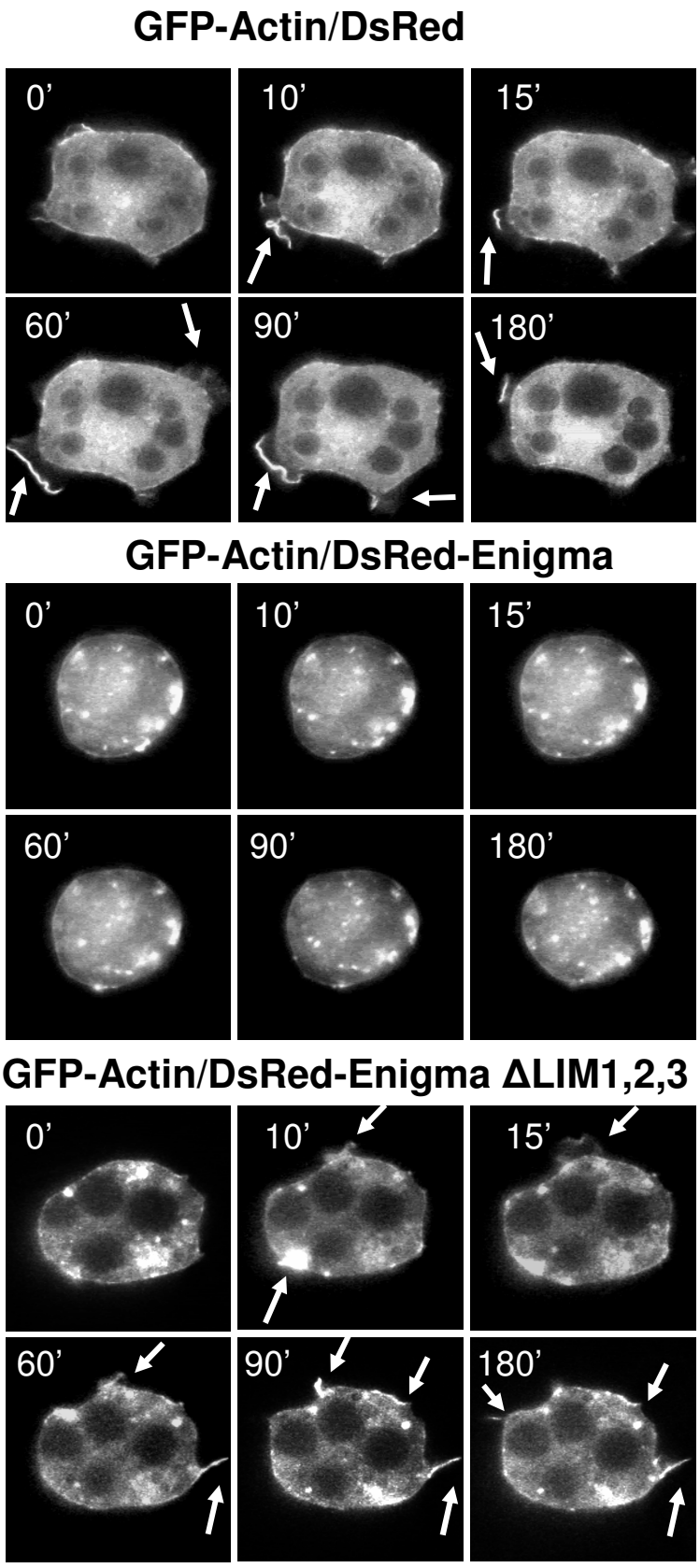

Fig 8.